Spectrochimica Acta Part A: Molecular and Biomolecular Spectroscopy 251 (2021) 119424

Contents lists available at ScienceDirect

Spectrochimica Acta Part A: Molecular and Biomolecular Spectroscopy

journal homepage: www.elsevier.com/locate/saa

Synthesis of 4-(4-ethyl-phenyl)-3-(4-methyl-phenyl)-1,2,4-oxadiazol-5(4*H*)-one and 4-(4-ethyl-phenyl)-3-(4-methyl-phenyl)-1,2,4-oxadiazole-5(4*H*)-thione and solvent effects on their infrared spectra in organic solvents

Yesim S. Kara [a,*], Mustafa Ünsal [a], Nalan Tekin [a], Aslı Eşme [b]

[a] *Kocaeli University, Science and Art Faculty, Department of Chemistry, Umuttepe Campus, 41001 Kocaeli, Turkey*
[b] *Kocaeli University, Department of Elementary Science Education, Umuttepe Campus, 41001 Kocaeli, Turkey*

HIGHLIGHTS

- Two novel oxadiazole ring derivatives were synthesized.
- The solvent effects were studied by Infrared spectroscopy.
- The theoretical results assigned using PED contributions.
- The ν(C=O), ν(C=N) and ν(C=S) were correlated with the Swain, AN, KBM and LSER.
- The quadratic and interactive effects of solvent parameters were also reported.

GRAPHICAL ABSTRACT

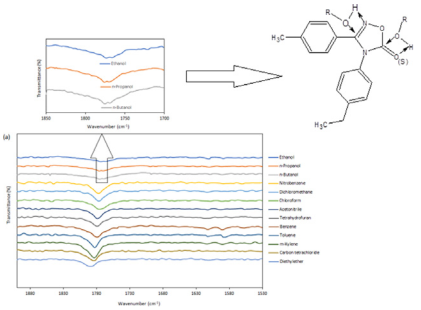

ARTICLE INFO

Article history:
Received 12 October 2020
Received in revised form 23 December 2020
Accepted 30 December 2020
Available online 5 January 2021

Keywords:
Infrared spectroscopy
Solvent effects
Oxadiazole ring
Empirical solvent parameters
Interaction effects
Quadratic equation

ABSTRACT

In the present study novel 4-(4-ethyl-phenyl)-3-(4-methyl-phenyl)-1,2,4-oxadiazol-5(4*H*)-one (compound (4)) and 4-(4-ethyl-phenyl)-3-(4-methyl-phenyl)-1,2,4-oxadiazole-5(4*H*)-thione (compound (5)) were synthesized. These oxadiazole ring derivatives were characterized by IR, ^{1}H NMR, ^{13}C NMR and HRMS analyses. The solvent effects on C=O, C=N and C=S stretching vibrational frequencies (ν(C=O), ν(C=N) and ν(C=S)) of synthesized compounds were investigated experimentally using attenuated total reflection (ATR) infrared spectroscopy and compared with the theoretical results assigned using the potential energy distribution (PED) contributions. Furthermore, the ν(C=O), ν(C=N) and ν(C=S) of compound (4) and compound (5) were correlated with empirical solvent parameters such as the solvent acceptor numbers, the Swain equation, the Kirkwood-Bauer-Magat equation, and the linear solvation energy relationships. Apart from the linear effects investigated in similar studies, solvent-induced vibrational shifts were investigated using the quadratic equation. The prediction capabilities of empirical solvent parameters were statistically compared. It was found that the linear solvation energy relationships show better correlation than the other empirical solvent parameters. Additionally, the quadratic equation provided more accurate predictions for the vibrational frequency locations than the Swain and the linear solvation energy relationships equations.

---

* Corresponding author.
E-mail address: yesimkara@kocaeli.edu.tr (Y.S. Kara).

https://doi.org/10.1016/j.saa.2020.119424
1386-1425/

1. Introduction

Oxadiazole ring is a heterocyclic aromatic compound including one oxygen and two nitrogen atoms in a five membered ring. Oxadiazoles may exist in four different isomeric structures such as 1,2,3-oxadiazole, 1,2,4-oxadiazole, 1,2,5-oxadiazole and 1,3,4-oxadiazole depending on the position of the nitrogen atoms in the ring [1]. The synthesis and biological activities of the molecules containing 1,2,4-oxadiazole ring stand as a continuously expanding area research in heterocyclic compounds which are commonly used in both pharmaceutical and agricultural fields. The 1,2,4-oxadiazole ring is generally present as fragments such as aromatic, non-aromatic rings and aliphatic structures in the structure of various drugs. Fig. 1 shows examples of drugs containing the 1,2,4-oxadiazole ring [2–7]. Therefore, it is predicted that investigating the solvent effects of heterocyclic compounds will yield valuable results both the academic and industrial communities [8].

Solvents effects are very important tools for pharmaceutical drug design because they affect the degree of absorption, transport and release of the drug in the organism [9]. The solvent effect can be studied by various spectroscopy methods, such as Infrared, NMR, Raman, Fluorescence and UV–Vis spectroscopy [10–14]. However, infrared spectroscopy is one of the oldest, well-established and inexpensive experimental techniques to study molecular vibrations, which are largely used to investigate solvent effects [10]. The infrared frequency shifts obtained of solute molecule in various dilute solutions show the interactions between solvent and solute [15].

Empirical solvent parameters are usually used to predict, correlate and characterize how solvent effects on spectral properties and describe and quantify of specific/nonspecific interactions between solvent and solute [16–19]. The most commonly used solvent parameters (single-parameter and multi-parameters) of to explore solvent effects on infrared spectra are the solvent acceptor number (AN) which was proposed by Gutman [20], the Kirkwood, Bauer and Magat (KBM) equation was presented by Kirkwood, Bauer and Magat [21,22], the Swain equation (SE) which includes the solvent parameters of *Aj* and *Bj* [23], and the linear solvation energy relationships (LSER) which includes the Kamlet-Taft's solvent parameters [24].

The KBM model equation is represented in Eq. (1) [25];

$$\frac{(\nu^0-\nu^s)}{\nu^0}=\frac{\Delta\nu}{\nu^0}=\frac{C(\varepsilon-1)}{(2\varepsilon+1)} \qquad (1)$$

where ε is the dielectric constant of solvent, C is a constant dependent on the electrical properties and dimensions of the vibrating solute dipole, ν^s and ν^o are the vibrational frequency of a solute in the solvent and the gas phase, respectively.

The solvent acceptor number (AN) equation is given in Eq. (2) [18],

$$\nu=\nu_0+K(AN) \qquad (2)$$

where K is the sensitivity of vibrational frequency (ν) to the solvent AN and ν_0 is the vibrational frequency of a solute in reference solvent.

The Swain equation is shown in Eq. (3) [16];

$$\nu=\nu_0+aA_j+bB_j \qquad (3)$$

where, ν and ν_0 are the vibration frequency of a solute in a solvent and the predicated vibration frequency in reference solvent, respectively. B_j and A_j are measure of the solvent hydrogen-bond acceptor basicity and hydrogen-bond donor acidity, respectively. The coefficients of b and a describe the sensitivity of solute for a solvent to the hydrogen-bond acceptor basicity and hydrogen-bond donor acidity, respectively.

The model equation of LSER is represented in Eq. (4) [16,26];

$$\nu=\nu_0+s\pi^*+a\alpha+b\beta \qquad (4)$$

where ν_0 and ν are the regression value of the stretching vibrational frequency in reference solvent and the stretching vibrational frequency of solute in pure solvent, respectively. β and α are a measure of the solvent hydrogen-bond acceptor basicity and hydrogen-bond donor acidity, respectively. π^* is an index of solvent dipolarity/polarizability. s, a and b in Eq. (4) are the regression coefficients and provide to the sensitivities of the stretching vibrational frequency of the organic compound to signify solvent parameters.

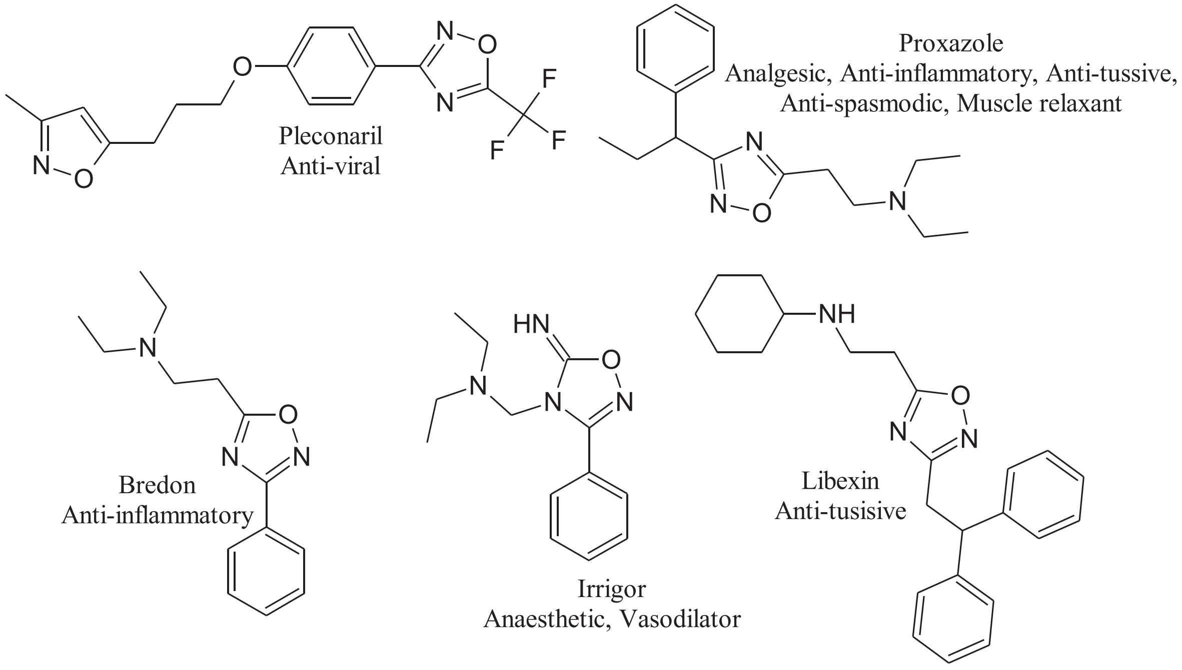

Fig. 1. Examples of drugs containing 1,2,4-oxadiazole ring.

During our literature review, it was seen that a number of studies were presented to develop a physically meaningful and quantitatively accurate description of vibration frequency changes and solute-solvent interactions [27,28]. To the best of our knowledge, experimental vibrational studies of 1,2,4-oxadiazole ring in different pure solvents has never been performed. In this study, two novel 1,2,4-oxadiazole derivative compounds were synthesized which were characterized by IR, ^{1}H NMR, ^{13}C NMR and HRMS analyses. In addition, the solvent effects on C=O, C=S and C=N stretching vibrational frequencies (ν(C=O), ν(C=N) and ν(C=S)) of the oxadiazole ring derivatives was studied experimentally using attenuated total reflection (ATR) infrared spectroscopy. The observed spectral results of the two novel 1,2,4-oxadiazole derivative compounds have been compared with the vibration assignments calculated with the help of the potential energy distribution (PED). The ν(C=O), ν(C=N) and ν(C=S) were correlated with the Swain, AN, KBM and LSER solvent scales. Additionally, the quadratic and interactive effects of solvent parameters on the experimental vibrational spectra of these oxadiazole ring derivatives were also investigated in this study.

2. Experimental procedure

The synthesis of 4-(4-ethyl-phenyl)-3-(4-methyl-phenyl)-1,2,4-oxadiazol-5(4*H*)-one, compound (4) and 4-(4-ethyl-phenyl)-3-(4-methyl-phenyl)-1,2,4-oxadiazole-5(4*H*)-thione, compound (5) is straightforward as illustrated in Scheme 1. Melting points of compound (4) and compound (5) were determined on Stuart SMP30 apparatus without a correction. The FT-IR spectra of compound (4) and compound (5) were recorded with Bruker Alpha II spectrometer in the region of 4000–400 cm^{-1}. The HRMS analyses were performed on Water SYNAPT G1 Mass Spectrometer. ^{1}H NMR and ^{13}C NMR spectra of compounds were recorded by Bruker Avance III (400 MHz) NMR spectrometer. The FTIR, ^{13}C NMR and ^{1}H NMR spectra for compound (4) and compound (5) were given in Supplementary Material.

All solvents obtained from the Merck Company used for solvent effect studies were of spectroscopic or analytical purity and distilled prior to the experiments. For the FT-IR solution spectra, the concentrations of compound (4) and compound (5) solutions were the range of 0.040 and 0.060 mol/L. The FT-IR spectra (4000–600 cm^{-1}) of the solutions were recorded using a Bruker Alpha II spectrophotometer with a resolution 2 cm^{-1} and 64 scans by Mercury-Cadmium-Telluride (MCT) detector. The solution FT-IR spectra were collected using a diamond ATR (Attenuated total reflection) at room temperature (20–23 °C). The FT-IR spectra of pure solvents as the background spectra, solid compound (4) and solid compound (5) were recorded under the same conditions. The Opus 6.5 software version was used for manipulation of all data stored on the computer.

3. Synthesis

4-methyl-benzaldehyde oxime (1), 4-methyl-benzimidoyl chloride (2) and 4-methyl-N-(4-ethyl-phenyl)benzamide oxime (3) were synthesized according to the literature. The methods in literature were applied with slight modifications for the synthesis of compound (4) and compound (5) (Scheme 1) [29].

3.1. Synthetic procedures

3.1.1. 4-(4-ethyl-phenyl)-3-(4-methyl-phenyl)-1,2,4-oxadiazol-5(4H)-one (Compound (4))

4-methyl-N-(4-ethyl-phenyl)benzamide oxime (3) (3.48 g, 13,6 mmol) was solved in xylene (15 mL) at room temperature with stirring. Triethylamine (1.52 g, 15 mmol) was added to the stirred solution and then ethyl chloroformate was added dropwise (1.47 g, 13,6 mmol) in xylene (10 mL) and the mixture was refluxed for 12 h. At the end of time, the reaction mixture was filtered whereby a filter paper and the solution was evaporated at reduced pressure. The crude reaction product was crystallized in ethyl acetate/petroleum ether (1:3) to give compound (4) (2.7 g, 72%); IR (KBr), ν (cm^{-1}): 1771.30 (C=O), 1593.85 (C=N); mp 123.5–125.0 °C; ^{1}H NMR (CDCl$_3$), δ (ppm) : 7.30–7.30 (dd, aromatic, 4H), 7.19–7.16 (dd, aromatic, 4H), 2.74–2.68 (q, —CH$_2$, 2H), 2.38 (s, —CH$_3$, 3H), 1.29–1.25 (t, —CH$_3$, 3H); ^{13}C NMR (CDCl$_3$), δ (ppm) : 158.64 (C=O), 157.61 (C=N), 145.94–120.20 (aromatic C) 28.53 (—CH$_2$), 21.55 (—CH$_3$), 15.21 (—CH$_3$). HRMS for $C_{17}H_{17}N_2O_2$ [M+H]$^+$ calculated 281.1290. Found 281.1290.

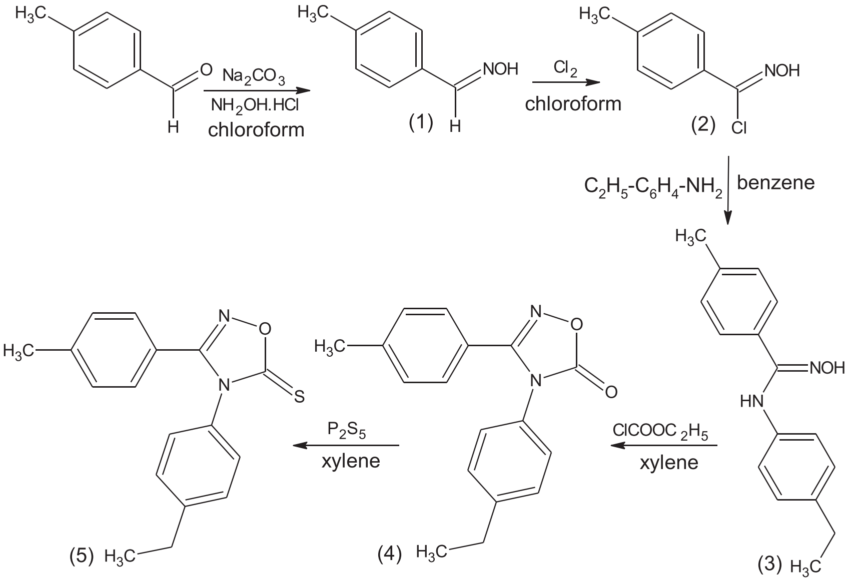

Scheme 1. Synthesis of 4-(4-ethyl-phenyl)-3-(4-methyl-phenyl)-1,2,4-oxadiazol-5(4*H*)-one and 4-(4-ethyl-phenyl)-3-(4-methyl-phenyl)-1,2,4-oxadiazole-5(4*H*)-thione.

3.1.2. 4-(4-ethyl-phenyl)-3-(4-methyl-phenyl)-1,2,4-oxadiazole-5 (4H)-thione (Compound (5))

Compound (4) (1.1 g, 4.33 mmol) was refluxed with P_2S_5 (0.466 g, 2 mmol) in xylene for 35 h. The reaction mixture was filtered through a filter paper and xylene was evaporated under reduced pressure. The crude product was purified by flash column chromatography, using ethyl acetate-petroleum ether (1:4) as eluent. The residue was crystallized from ethanol. (R_f: 0.55). The product recrystallized from ethanol to give compound (5) (0.49 g, Yield 40%; IR (KBr), ν (cm^{-1}): 1590.95 (C=N), 1327.10 (C=S); mp 172–173.3 °C; ^{1}H NMR (CDCl$_3$), δ (ppm) : 7.36–7.34 (d, aromatic, 2H), 7.25–7.16 (m, aromatic, 6H), 2.77–2.72 (q, —CH$_2$, 2H), 2.37 (s, —CH$_3$, 3H), 1.32–1.28 (t, —CH$_3$, 3H); ^{13}C NMR (CDCl$_3$), δ (ppm) : 187.47(C=S), 158.85 (C=N), 146.72–118.81 (aromatic C) 28.56 (—CH$_2$), 21.56 (—CH$_3$), 14.99 (—CH$_3$). HRMS for $C_{17}H_{17}N_2OS$ [M+H]$^+$ calculated 297.1062. Found 297.1060.

3.2. Computational procedures

The theoretical computations were carried out using the Gaussian 09 Rev. A. 11.4 [30] program with the density functional theory (B3LYP functional; Becke, 3-parameter, Lee–Yang-Parr) [31,32] at the 6-31G(d,p) basis set. The compound (4) and compound (5) were viewed using GaussView 5.0.8 [33]. The experimentally predicted results of the compound (4) and compound (5) in 13 different polar or non-polar solvents have compared with the theoretical C=O, C=N and C=S stretching vibrational frequencies, together with the potential energy distribution (PED) contributions interpreted using the VEDA 4 program [34]. The computed wavenumbers scaled by 0.9608 were calculated by the DFT/B3LYP/6-31G (d,p) level of theory [35].

4. Results and discussion

4.1. Solvent effects on the experimental vibrational spectra of compound (4) and compound (5)

The experimental ν(C=O)/ν(C=N) of compound (4) and ν(C=S)/ν(C=N) of compound (5) in 13 different pure solvents and the solvent parameters are presented in Table 1. For compound (4) and compound (5), the experimental stretching vibrational frequencies are determined at higher frequency in less polar or apolar solvents whereas the vibrational frequency bands of the compounds were observed at lower frequencies in polar solvents. Fig. 2(a) and (b) display the experimental FT-IR spectra of compound (4) and compound (5) in the solvents. Additionally, Fig. 2(a) and (b) show the frequency shifts and changes in the IR intensity of vibration frequencies of compound (4) and compound (5) from the polar solvents to the apolar solvents.

In FTIR spectra of compound (4), one C=O absorption band in non-alcohol solvents and two C=O absorption bands in ethanol, n-propanol and n-butanol were determined. This observation can be explained due to the occurrence of two types ν(C=O) of compound (4) in alcohol solvents and possibility for alcohol molecules for self-associate to form large cluster-like molecules by acting as both a H-bond donor and a H-bond acceptor of their hydroxyl group [25]. The H-bonds can form between ν(C=O) of compound (4) with the self-associated or free alcohol molecules. Therefore, the electron density of C=O in compound (4) decreases and two C=O absorption bands are observed [25]. Similar observation has been reported in the literature [25]. In this study, it was reported that the carbonyl group and alcohol can make hydrogen bonds in three different ways. It was explained that the carbonyl group, monomer alcohol and dimer (self-associated) alcohols can interact, and the third type of hydrogen bonding can be connected with the monomer alcohol of each unpaired electron pair in the carbonyl group separately. It was proposed that Band I could be the effect of hydrogen bonds and Band II could be referred to non-specific interactions (i.e. van der Waals forces) between the investigated molecule and alcohol solvents.

A comparison of the experimental wavenumbers along with the computed wavenumbers using the DFT/B3LYP/6-31G(d,p) level of theory with their potential energy distributions (PED) of the compound (4) and compound (5) in the polar and non-polar solvents were also listed in Table 1. Almost all carbonyl ν(C=O) stretching vibrations have a very intense and narrow peak in the range of 1800–1600 cm^{-1} [36,37]. This experimental/theoretical ν(C=O) bands were found at lower frequencies 1779.02–1782.03 cm^{-1}/1771.94–1779.27 cm^{-1} (with 84% pure PED contributions) in polar solvents such as acetonitrile, nitrobenzene, ethanol, n-propanol, n-butanol, dichloromethane, tetrahydrofuran and at higher frequencies 1779.02–1785.50 cm^{-1}/1783.14–1794.09 cm^{-1} (with 84% pure PED contributions) in non-polar solvents such as chloroform, diethylether, m-xylene, toluene, benzene, carbon tetrachloride, respectively.

The bands due to C=N stretching modes of 1,3,4 oxadiazole ring are reported at 1553, 1538, 1497, 1490 cm^{-1} (FT-IR), 1572, 1550, 1492, 1490 cm^{-1} (DFT) by Bee et al. [38]. The calculated frequencies of the ν(C=N) stretching vibrations for compound (4)/compound (5) are identified at 1571.55–1572.42 cm^{-1} (23–24%), 1533.75–1534.22 cm^{-1} (34–35%)/1569.48–1570.60 cm^{-1} (11–14%), 1534.43–1533.24 cm^{-1} (33–34%) in polar solvents and at 1573.36–1574.47 cm^{-1} (24–25%), 1535.08–1536.05 cm^{-1} (35%)/1571.12–1572.40 cm^{-1} (15–18%), 1533.54–1534.45 (33%) cm^{-1} in non-polar solvents.

The C=S group is less polar than the C=O group and the C=S stretching vibration attached to an N atom is found over the wide range of 1563–700 cm^{-1} [39]. The wavenumbers computed at 1270.52–1272.70 cm^{-1} (18–19%) and 1273.90–1276.29 cm^{-1} (16–18%) using the DFT/B3LYP/6-31G(d,p) level of theory are assigned to *ν*(C=S) stretching modes for compound (5), the recorded wavenumber for this *ν*(C=S) mode in the FT-IR spectrum at 1334.14–1336.15 cm^{-1} and 1337.17–1345.68 cm^{-1} in polar and non-polar solvents, respectively.

Fig. 3. illustrates the expected interactions between the studied 1,2,4-oxadiazole derivatives and the alcohols. Since there is no α hydrogen in the molecules studied, it is thought that the partially positively charged carbon in the C = X (X: O, N, S) bond and using alcohol serve as a hydrogen bond donor. Due to its molecular structure, the C=N group is sterically disabled compared to the C=O and C=S groups, so its interaction with alcohol is limited. This result can be seen in the correlation coefficients of *Aj* and α.

The experimental the ν(C=O), ν(C=N) and ν(C=S) of compound (4) and compound (5) were correlated with empirical solvent parameters such as the Ans, the KBM equation, the SE, and the LSER. The KBM, ANs, Swain and LSER equations of the solvent-induced the ν(C=O), ν(C=N) and ν(C=S) and correlation coefficients are listed in Table 2 for compound (4) and Table 3 for compound (5).

Fig. 4(a–g) is plots of the ν(C=O)/ν(C=N) of compound (4) and the ν(C=S)/ν(C=N) of compound (5) versus $\frac{(\varepsilon-1)}{2\varepsilon+1}$ of the KBM equation. The negative slopes of the plots show that the ν(C=O)/ν(C=N) of compound (4) and the ν(C=S)/ν(C=N) of compound (5) are red-shifted with the increase of the solvent dielectric constant. The linear equation parameters and correlation coefficients for compounds (4) and compound (5) are shown in Table 2 and Table 3, respectively. It is found that a poor relationship exists between the KBM parameters with the ν(C=O)/ν(C=N) of compound (4) and the ν(C=S)/ν(C=N) of compound (5) (Table 2 and Table 3) since the frequency shifts are not only depended on the dielectric

Table 1
The ν(C=O)/ν(C=N) of compound (4) and ν(C=S)/ν(C=N) of compound (5) in different solvents and solvent parameters.

Solvent		Compound (4)				Compound (5)				Solvent Parameters							
		ν(C=O)$_1$	ν(C=O)$_2$	ν(C=N)$_1$	ν(C=N)$_2$	ν(C=S)$_1$	ν(C=S)$_2$	ν(C=N)$_1$	ν(C=N)$_2$	*ε*	*f(ε)*[a]	*AN*	*β*	*α*	*π**	*A$_j$*	*B$_j$*
Acetonitrile	**Exp.**	1779.02	–	1613.51	1592.52	1334.14	1310.50	1612.88	1601.82	35.94	0.479	18.9	0.40	0.19	0.66	0.37	0.86
	Theo.	1771.94 (84%)	–	1571.55 (23%)	1533.75 (35%)	1270.52 (18%)		1569.48 (13%)	1534.43 (34%)								
Nitrobenzene	**Exp.**	1777.07	–	1612.78	1591.80	1336.22	1311.65	1614.59	1602.67	34.78	0.478	14.8	0.30	0	0.86	0.29	0.86
	Theo.	1771.99 (84%)	–	1571.56 (23%)	1533.73 (35%)	1270.53 (18%)		1569.49 (11%)	1534.42 (33%)								
Ethanol	**Exp.**	1769.54	1774.52	1607.67	1586.09	1330.79	1304.55	1608.76	1592.45	24.55	0.470	37.1	0.75	0.86	0.54	0.66	0.45
	Theo.	1772.84 (84%)		1571.65 (23%)	1533.82 (35%)	1270.80 (18%)		1569.59 (11%)	1534.23 (33%)								
n-Propanol	**Exp.**	1771.72	1777.80	1609.26	1587.24	1331.14	1306.17	1610.51	1594.46	20.45	0.464	33.7	0.90	0.84	0.52	0.63	0.44
	Theo.	1773.44 (84%)		1571.33 (23%)	1535.20 (34%)	1271.09 (19%)		1569.96 (13%)	1532.99 (33%)								
n-Butanol	**Exp.**	1770.96	1785.39	1610.02	1589.52	1332.99	1307.86	1611.49	1596.31	17.51	0.458	32.2	0.84	0.84	0.47	0.61	0.43
	Theo.	1774.12 (84%)		1571.80 (23%)	1533.88 (35%)	1271.29 (19%)		1570.02 (13%)	1532.99 (33%)								
Dichloromethane	**Exp.**	1777.07		1612.78	1590.35	1333.62	1310.22	1613.01	1599.54	8.93	0.420	20.4	0.10	0.13	0.82	0.33	0.80
	Theo.	1777.82 (84%)		1572.23 (24%)	1534.10 (35%)	1272.31 (18%)		1570.44 (14%)	1533.16 (33%)								
Tetrahydrofuran	**Exp.**	1782.03		1614.09	1592.10	1336.15	1310.83	1614.12	1601.22	7.58	0.407	8.0	0.55	0	0.55	0.17	0.67
	Theo.	1779.27 (84%)		1572.42 (24%)	1534.22 (35%)	1272.70 (18%)		1570.60 (14%)	1533.24 (33%)								
Chloroform	**Exp.**	1779.02		1613.34	1593.15	1337.17	1311.64	1615.85	1603.09	4.89	0.361	23.1	0.10	0.20	0.58	0.42	0.73
	Theo.	1783.14 (84%)		1573.36 (24%)	1535.08 (35%)	1273.90 (18%)		1571.12 (15%)	1533.54 (33%)								
Diethylether	**Exp.**	1789.01		1615.09	1595.21	1338.59	1313.77	1615.14	1604.50	4.20	0.340	3.9	0.47	0	0.24	0.12	0.34
	Theo.	1784.43 (84%)		1573.52 (24%)	1535.18 (35%)	1274.14 (18%)		1571.13 (15%)	1534.12 (33%)								
m-Xylene	**Exp.**	1784.52		1616.84	1596.05	1341.26	1313.20	1616.90	1604.42	2.37	0.239	2.4	0.12	0	0.47	0.06	0.50
	Theo.	1793.15 (84%)		1574.39 (25%)	1536.00 (35%)	1276.12 (16%)		1572.30 (17%)	1534.33 (33%)								
Toluene	**Exp.**	1784.48		1614.32	1595.07	1342.83	1314.18	1617.46	1605.04	2.38	0.240	6.8	0.11	0	0.49	0.13	0.54
	Theo.	1793.01 (84%)		1574.35 (25%)	1535.96 (35%)	1276.08 (16%)		1572.27 (17%)	1534.35 (33%)								
Benzene	**Exp.**	1783.65		1616.81	1596.05	1343.16	1315.52	1617.35	1605.61	2.27	0.229	8.2	0.10	0	0.55	0.15	0.59
	Theo.	1793.81 (84%)		1574.43 (25%)	1536.06 (35%)	1276.22 (16%)		1572.37 (18%)	1534.42 (33%)								
Carbon tetrachloride	**Exp.**	1785.50		1617.64	1597.71	1345.68	1316.31	1618.69	1608.76	2.24	0.226	8.6	0.10	0	0.21	0.09	0.34
	Theo.	1794.09 (84%)		1574.47 (25%)	1536.05 (35%)	1276.29 (16%)		1572.40 (18%)	1534.45 (33%)								

The unit of the stretching vibrational frequency is cm^{-1}.

[a] $f(\varepsilon) = (\varepsilon - 1)/(2\varepsilon + 1)$.

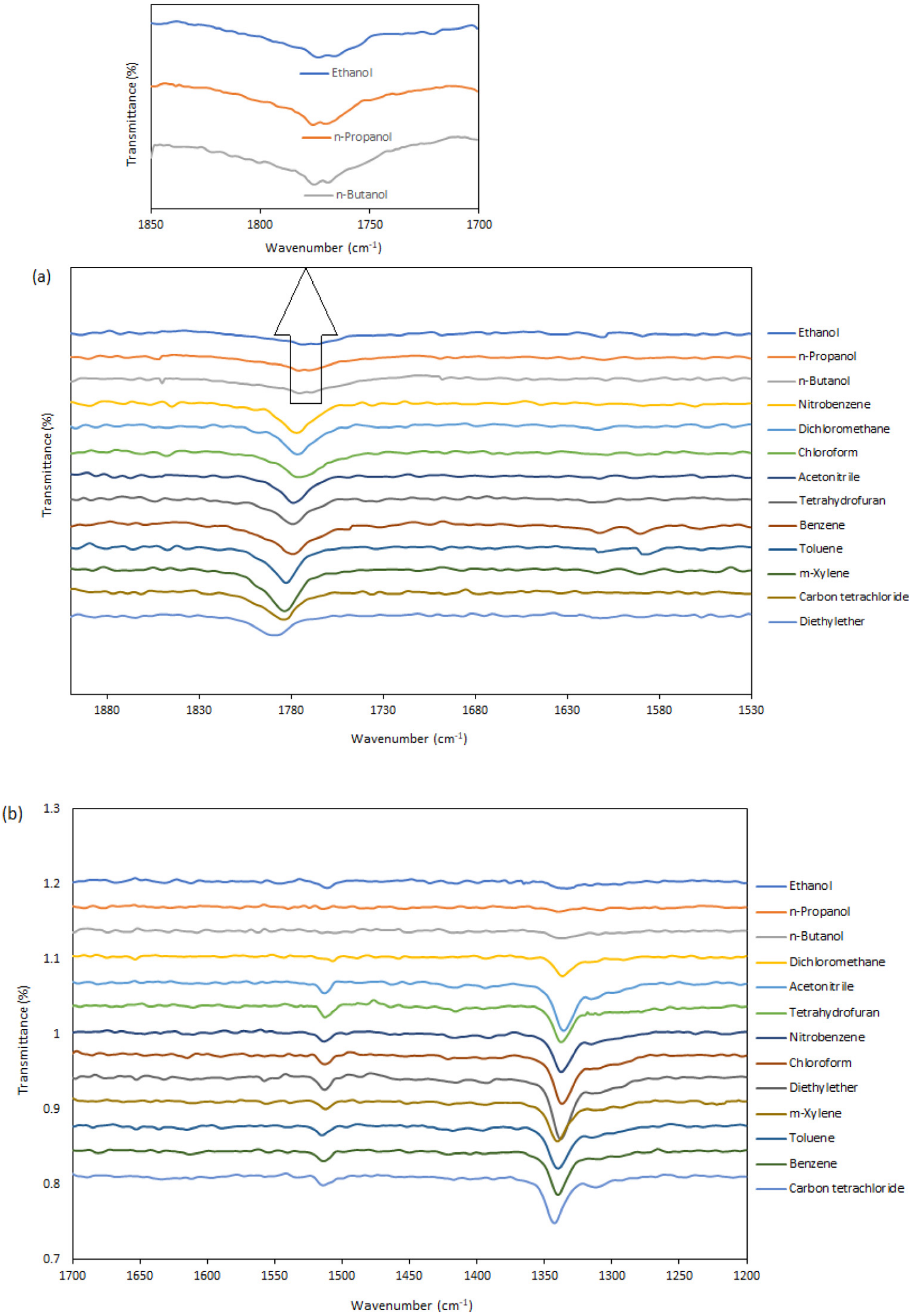

Fig. 2. FTIR spectra of compound (4) and compound (5) in solvents.

constant of solvent. The observation can be explained that the consideration of only dielectric constants in KBM equation and the formation of molecular complexes between solvents with compounds (4) and compound (5) [40]. According to this result, in order to explain the shifts of the ν(C=O)/ν(C=N) and the ν(C=S)/ν(C=N) in different solvents, more effects such as hydrogen bonding, non-specific interactions and steric effects must be considered. Thus, KBM equation containing the single parameter is not sufficient to generally explain of solvent effects on the ν(C=O)/ν(C=N) of compound (4) and the ν(C=S)/ν(C=N) of compound (5). Similar results were reported for the correlation of the experimental stretching vibrational frequencies with the KBM equation [25,41].

Fig. 5(a–g) exhibits the plots of the ν(C=O)/ν(C=N) of compound (4) and the ν(C=S)/ν(C=N) of compound (5) vs. the solvent ANs. The linear equation parameters and correlation coefficients for compound (4) and compound (5) are shown in Table 2 and Table 3, respectively. It is shown that there is a poor correlation between the ν(C=O)/ν(C=N) of compound (4) and the ν(C=S)/ν(C=N) of compound (5) with the solvent ANs due to a role of solvents. It was also found that when the solvent ANs which indicates

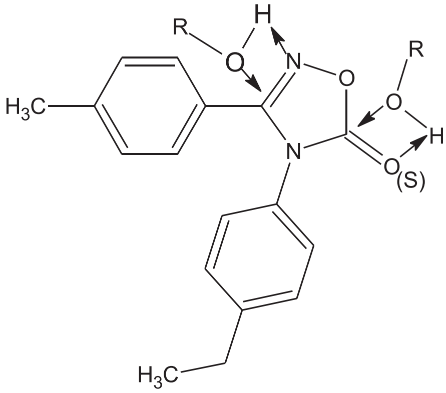

Fig. 3. Expected interaction between studied 1,2,4-oxadiazole derivatives and alcohol.

Table 2
Solvent equations for compound (4).

Stretching Vibrational Frequency	Equation	R^2
	KBM Equation	
$\nu(C{=}O)_1$	1796.20 - 45.05 f(μ)	0.5934
$\nu(C{=}N)_1$	1622.03 - 23.32 f(μ)	0.6562
$\nu(C{=}N)_2$	1603.20 - 28.70 f(μ)	0.7161
	AN Equation	
$\nu(C{=}O)_1$	1787.70 - 0.49 AN	0.9060
$\nu(C{=}N)_1$	1617.30 - 0.23 AN	0.8365
$\nu(C{=}N)_2$	1597.00 - 0.27 AN	0.7967
	Swain Equation	
$\nu(C{=}O)_1$	$1790.20 - 26.77\ A_j - 3.81\ B_j$	0.9128
$\nu(C{=}N)_1$	$1617.43 - 13.07\ A_j + 0.03\ B_j$	0.8809
$\nu(C{=}N)_2$	$1598.14 - 14.90\ A_j - 1.71\ B_j$	0.8363
	LSER Equation	
$\nu(C{=}O)_1$	$1790.72 - 14.71\pi^* - 15.51\alpha + 0.85\beta$	0.9695
$\nu(C{=}N)_1$	$1618.76 - 5.70\pi^* - 5.45\alpha - 2.75\beta$	0.9076
$\nu(C{=}N)_2$	$1600.05 - 8.78\pi^* - 5.29\alpha - 4.23\beta$	0.9247

The unit of the stretching vibrational frequency is cm^{-1}.

Table 3
Solvent equations for compound (5).

Stretching Vibrational Frequency	Equation	R^2
	KBM Equation	
$\nu(C{=}S)_1$	1353.20 - 43.13 f(μ)	0.8727
$\nu(C{=}S)_2$	1321.50 - 27.67 f(μ)	0.6780
$\nu(C{=}N)_1$	1623.50 - 24.66 f(μ)	0.7526
$\nu(C{=}N)_2$	1614.50 - 34.93 f(μ)	0.5969
	AN Equation	
$\nu(C{=}S)_1$	1342.80 - 0.33 AN	0.6678
$\nu(C{=}S)_2$	1315.70 - 0.26 AN	0.7882
$\nu(C{=}N)_1$	1617.90 - 0.21 AN	0.7251
$\nu(C{=}N)_2$	1607.40 - 0.35 AN	0.7749
	Swain Equation	
$\nu(C{=}S)_1$	$1346.47 - 19.07\ A_j - 5.76\ B_j$	0.7855
$\nu(C{=}S)_2$	$1316.06 - 14.83\ A_j - 0.34\ B_j$	0.8337
$\nu(C{=}N)_1$	$1618.36 - 12.13\ A_j - 0.41\ B_j$	0.7798
$\nu(C{=}N)_2$	$1606.97 - 19.80\ A_j + 1.21\ B_j$	0.8203
	LSER Equation	
$\nu(C{=}S)_1$	$1348.65 - 13.52\pi^* - 3.56\alpha - 9.03\beta$	0.8660
$\nu(C{=}S)_2$	$1317.78 - 6.81\pi^* - 5.65\alpha - 4.15\beta$	0.9142
$\nu(C{=}N)_1$	$1620.24 - 5.89\pi^* - 3.26\alpha - 5.23\beta$	0.8965
$\nu(C{=}N)_2$	$1609.94 - 8.50\pi^* - 8.10\alpha - 5.24\beta$	0.9281

The unit of the stretching vibrational frequency is cm^{-1}.

electrophilicity of the solvent increases, the $\nu(C{=}O)/\nu(C{=}N)$ of compound (4) and the $\nu(C{=}S)/\nu(C{=}N)$ of compound (5) shifts to lower frequencies (Table 1) and this trend verifies the presence of some specific interaction between compound (4) and compound (5) with polar solvents [40]. According to the results, the solvent ANs do not play an important role in determining solvent-induced vibrational shifts in this study and the contribution of polarization effects must also be considered.

In the investigation of solvent-induced frequency shifts, specific solvent effects such as H-bond and electron pair transfer are described using Swain equations [42]. The Swain equations for the $\nu(C{=}O)/\nu(C{=}N)$ of compound (4) and the $\nu(C{=}S)/\nu(C{=}N)$ of compound (5) were given in Table 2. The correlation of the Swain equations for the $\nu(C{=}O)/\nu(C{=}N)$ of compound (4) and the $\nu(C{=}S)/\nu(C{=}N)$ of compound (5) are good and better than that of ANs of the solvents due to considering both the Lewis basicity and acidity for the solvents. The negative signs determined for the coefficients of A_j and B_j show that the increase of hydrogen bond donor acidity and hydrogen bond acceptor basicity of the solvent leads to red-shift of the $\nu(C{=}O)/\nu(C{=}N)$ of compound (4) and the $\nu(C{=}S)/\nu(C{=}N)$ of compound (5). However, the coefficients of B_j were determined as positive for $\nu(C{=}N)_1$ of compound (4) and $\nu(C{=}N)_2$ of compound (5). This observation can be explained by the fact that the increase in solvent hydrogen bond acceptor basicity in studied this functional groups causes an increase in electron density and the measured vibration frequencies is blue-shifted. It was observed in Table 1 that the measured $\nu(C{=}N)_1$ of compound (4) and $\nu(C{=}N)_2$ of compound (5) tended to increase as the coefficients *Bj* increased. As a result, it can be said that the tendency to blue shift is not as strong as the red shift.

The C=O, C=N and C=S groups in compound (4) and compound (5) are a hydrogen bond acceptor. The solvents tend to donate proton and form H-bond with the C=O, C=N and C=S groups in compound (4) and compound (5) with the increase of solvent hydrogen bond donor acidity. Consequently, there is a decrease in the electron density of the C=O, C=N and C=S groups and the $\nu(C{=}O)/\nu(C{=}N)$ and the $\nu(C{=}S)/\nu(C{=}N)$ are red-shifted. By comparing the coefficients of A_j and B_j, it was found that the red-shift of the $\nu(C{=}O)/\nu(C{=}N)$ of compound (4) and the $\nu(C{=}S)/\nu(C{=}N)$ of compound (5) band induced by hydrogen bond donor acidity is larger than the one induced by hydrogen bond acceptor basicity of the solvent since the coefficients of A_j are much larger than the coefficients of B_j. As a result, the stretch vibration frequencies of C=O/C=N and C=S/C=N functional groups are more sensitive to solvent hydrogen bond donor acidity than solvent hydrogen bond acceptor basicity because of the unpaired electrons they have. The success of SE applied to FT-IR spectroscopy for the $\nu(C{=}O)/\nu(C{=}N)$ of compound (4) and the $\nu(C{=}S)/\nu(C{=}N)$ of compound (5) are shown in Fig. 6.

The determined LSER parameters are given in Table 2 and Table 3 for compound (4) and compound (5), respectively. The results obtained using LSER equation exhibit better correlations than that of the KBM equation, ANs and SE since the LSER model takes into account not only the specific interaction parameters such as α and β but also the non-specific interaction parameter like π^* in order to explain the position shifts of the C=O/C=N and the C=S/C=N bands [41,42]. The negative coefficients of π^* inform that red-shifted of the $\nu(C{=}O)/\nu(C{=}N)$ and the $\nu(C{=}S)/\nu(C{=}N)$ is induced by non-specific solvent effects. This situation may be due to the decreasing electron density. The coefficients of π^* determined from LSER equation which have the biggest absolute values compared to other parameters prove that non-specific solvent effects are dominant in the compound/solvent interactions. The coefficients of α and β are also negative similar to the results of the coefficients of A_j and B_j parameters in SE. This states the same influence concerning the red-shift of the $\nu(C{=}O)/\nu(C{=}N)$ and the ν

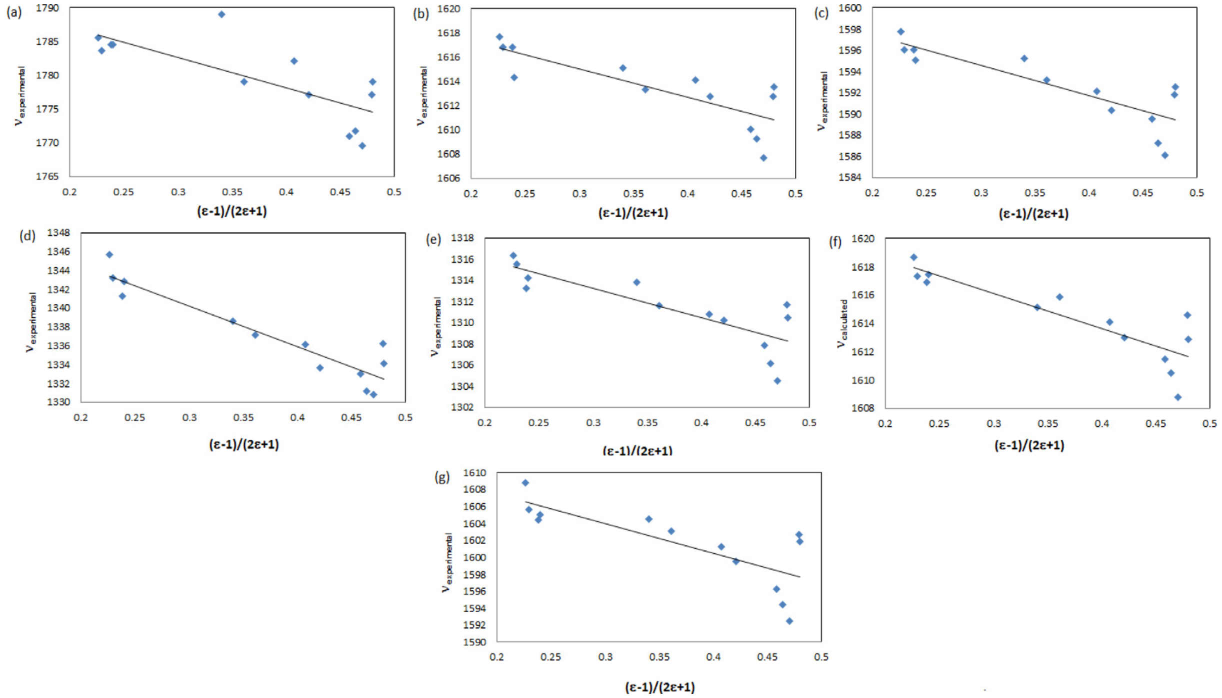

Fig. 4. Plots of KBM parameter vs. **(a)** ν(C=O)$_1$, **(b)** ν(C=N)$_1$, and **(c)** ν(C=N)$_2$ of compound (4) and vs. **(d)** ν(C=S)$_1$, **(e)** ν(C=S)$_2$, **(f)** ν(C=N)$_1$, and **(g)** ν(C=N)$_2$ of compound (5).

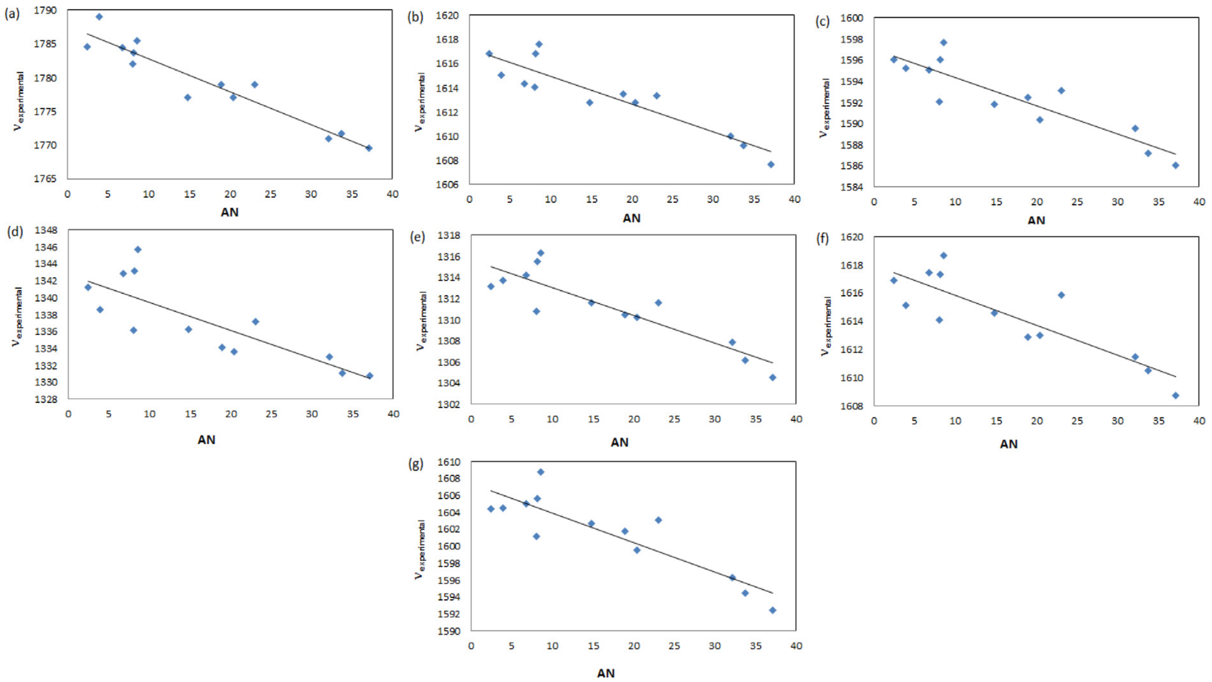

Fig. 5. Plots of AN parameters vs. **(a)** ν(C=O)$_1$, **(b)** ν(C=N)$_1$, and **(c)** ν(C=N)$_2$ of compound (4) and vs. **(d)** ν(C=S)$_1$, **(e)** ν(C=S)$_2$, **(f)** ν(C=N)$_1$, and **(g)** ν(C=N)$_2$ of compound (5).

(C=S)/ν(C=N) by hydrogen bond acceptor basicity and hydrogen band donor acidity of the solvent. However, the coefficient of α is slightly bigger than the coefficient of π^* and the coefficient of β were determined as positive for ν(C=O)$_1$ of compound (4). The result can be explained as follows: Since the four unpaired electrons on the oxygen atom of C=O group form hydrogen bonds, its contribution to the solvent effect is more dominant than the dipolarity/polarizability effect of the solvent.

The coefficients of α are bigger than the coefficients of β except ν(C=S)$_1$ and ν(C=N)$_1$ for compound (5). When the 1,2,4-oxadiazole derivatives are examined, it can be easily seen that the hydrogen bond acceptor group properties of these molecules are dominant due to the unpaired electrons. Also, the hydrogen bond donor group properties of molecules are very weak since they do not contain polarized H atoms. Therefore, the ν(C=O)/ν(C=N) of compound (4) and the ν(C=S)/ν(C=N) of compound (5) are more

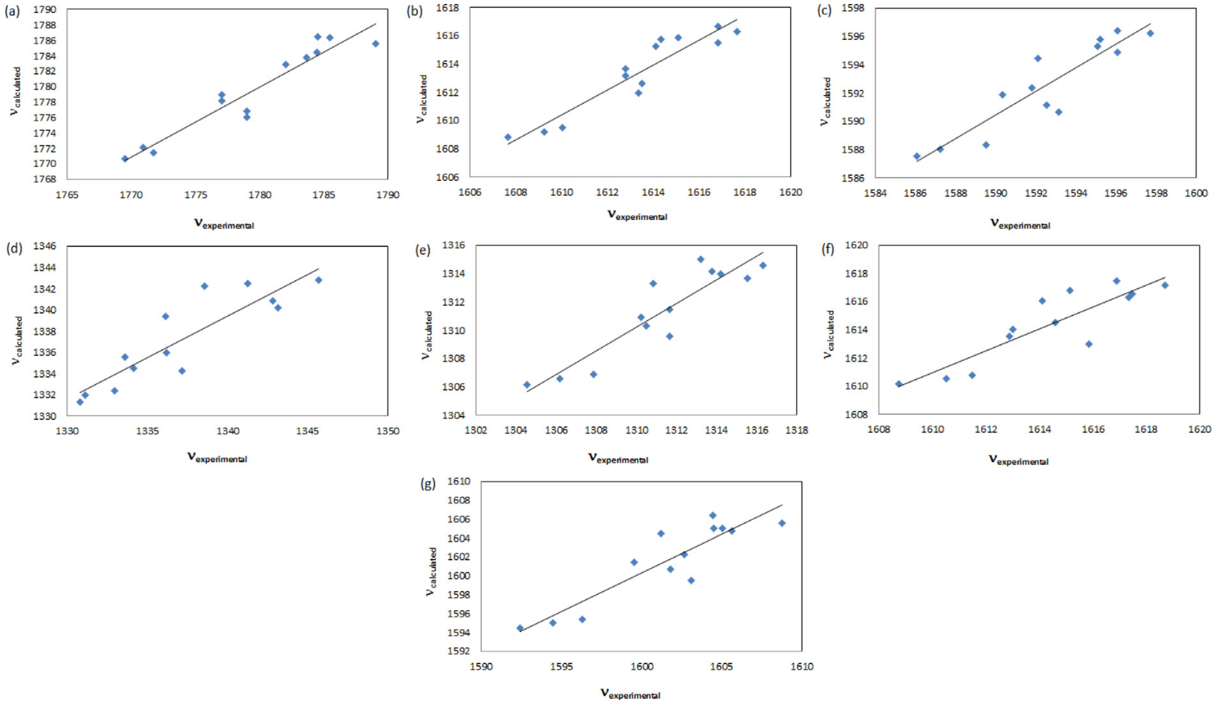

Fig. 6. Calculated **(a)** ν(C=O)$_1$ **(b)** ν(C=N)$_1$ **(c)** ν(C=N)$_2$ of compound (4) and **(d)** ν(C=S)$_1$, **(e)** ν(C=S)$_2$, **(f)** ν(C=N)$_1$, and **(g)** ν(C=N)$_2$ of compound (5) by using SE vs. experimental values.

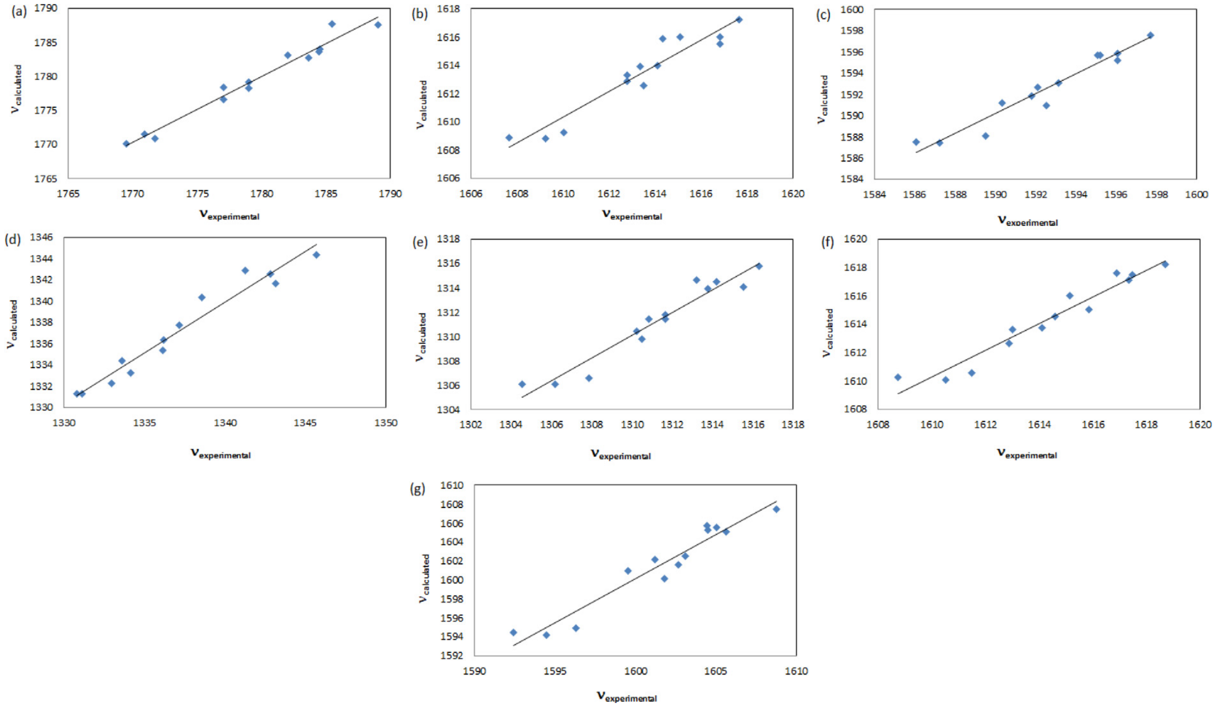

Fig. 7. Calculated **(a)** ν(C=O)$_1$ **(b)** ν(C=N)$_1$ **(c)** ν(C=N)$_2$ of compound (4) and **(d)** ν(C=S)$_1$, **(e)** ν(C=S)$_2$, **(f)** ν(C=N)$_1$, and **(g)** ν(C=N)$_2$ of compound (5) using LSER equation vs. experimental values.

sensitive to hydrogen bond donor acidity of solvents than hydrogen band acceptor basicity.

The ν(C=O)/ν(C=N) of compound (4) and the ν(C=S)/ν(C=N) of compound (5) achieve very good correlations with the parameters of LSER equations. It is suggested that non-specific solvent effects between solvents with compound (4) and compound (5) play an important role because of the biggest coefficient value of π^*. As compared to other solvent scales such as the KBM equation, ANs and SE, the LSER equation provides physically meaningful and a quantitatively accurate explanation of vibrational frequency shifts caused by the solute and solvent interactions in both polar and non-polar solvents. The success of LSER equation applied to FT-IR spectroscopy for the ν(C=O)/ν(C=N) of compound (4) and the ν(C=S)/ν(C=N) of compound (5) are show in Fig. 7.

Table 4
Regression model results for SE.

Term	Coefficient	Standard Error	t	F	P	R^2
Compound (4)						
ν(C=O)$_1$						0.9488
Constant	1798.50	3.75	479.93	55.55	0.000	
A_j	−54.30	11.20	−4.86	23.66	0.001	
B_j	−22.23	7.74	−2.87	8.26	0.018	
A_jB_j	59.50	23.70	2.51	6.32	0.033	
Compound (5)						
ν(C=N)$_2$						0.8887
Constant	1616.01	4.27	378.45	23.95	0.000	
A_j	−49.20	12.70	−3.86	14.93	0.004	
B_j	−18.43	8.81	−2.09	4.37	0.066	
A_jB_j	63.50	27.00	2.35	5.53	0.043	

The unit of the stretching vibrational frequency is cm^{-1}.

4.2. Interactive effects of solvent parameters on the experimental vibrational spectra of compound (4) and compound (5)

The Swain and LSER equations are commonly used to describe the effects of solvent on vibrational spectra of organic molecules. The Swain and LSER equations are multi-parameter equations and include the main effects of solvent parameters such as A_j, B_j, π^*, α and β on the vibrational spectra. In this study, apart from the linear effects investigated in similar studies, the linear, interactive and quadratic effects of the solvent parameters were also studied. The quadratic and interactive effects of solvent parameters were determined using multiparameter regression by MINITAB 19 (USA).

The solvent effects on the ν(C=O)/ν(C=N) of compound (4) and the ν(C=S)/ν(C=N) of compound (5) for SE were explained by the following Eq. (5) including quadratic and interactive effects of solvent parameters:

$$\nu = \nu_0 + \beta_1 A_j + \beta_2 B_j + \beta_{11} A_j^2 + \beta_{22} B_j^2 + \beta_{12} A_j B_j \tag{5}$$

In Eq. (5), the predicted frequency (ν) was correlated to the intercept (ν_0), linear (β_1, β_2), quadratic (β_{11}, β_{22}) and interaction (β_{12}) coefficients. Coefficients of the respective effects were represented by β and were determined by applying a Student's *t*-test. The Minitab 19 was used for graphical analysis and multi-linear regression of the ν(C=O)/ν(C=N) of compound (4) and the ν(C=S)/ν(C=N) of compound (5). The regression coefficient, standard deviation of each coefficient, P values and t values for all the linear, interaction and quadratic effects of the parameter determined from analysis of the data was displayed in Table 4 for SE.

As can be seen from Table 4, only ν(C=O)$_1$ of compound (4) and ν(C=N)$_2$ of compound (5) respond to the quadratic and interaction effects of solvent parameter. The coefficients of determination (0.9488 for ν(C=O)$_1$ of compound (4) and 0.8887 for ν(C=N)$_2$ of compound (5)) obtained from the model containing the linear, quadratic and interaction effects are bigger than that of the linear model (0.9128 for ν(C=O)$_1$ of compound (4) and 0.8203 for ν(C=N)$_2$ of compound (5)) given in Table 2 and Table 3. Therefore, it was found that the model including the linear, interaction and quadratic effects is the most appropriate model for ν(C=O)$_1$ of compound (4) and ν(C=N)$_2$ of compound (5) and shows a better correlation compared to the linear model.

The regression equations for the ν(C=O)$_1$ of compound (4) and ν(C=N)$_2$ of compound (5) is given in Eqs. (6) and (7), respectively:

$$\nu_{(C=O)_1} = 1798.50 - 54.30A_j - 22.23B_j + 59.50A_jB_j \tag{6}$$

$$\nu_{(C=N)_2} = 1616.01 - 49.20A_j - 18.43B_j + 63.50A_jB_j \tag{7}$$

The smaller the value of P and larger the values of t and F indicate that the model is statistically significant (with 95% confidence level) [43]. It was found that the linear effects of A_j (P = 0.001) and B_j (P = 0.018) on ν(C=O)$_1$ of compound (4) are highly significant. The linear effect of A_j (P = 0.004) on ν(C=N)$_2$ of compound (5) are highly significant whereas B_j (P = 0.066) are not significant. Additionally, it was observed that interaction effect of A_j and B_j are slightly significant for ν(C=O)$_1$ of compound (4) (P = 0.033) and ν(C=N)$_2$ of compound (5) (P = 0.043). According to the results, the interaction effect of A_j and B_j are considered as slightly significant factor for the ν(C=O)$_1$ of compound (4) and ν(C=N)$_2$ of compound (5).

The solvent effects on the ν(C=O)/ν(C=N) of compound (4) and the ν(C=S)/ν(C=N) of compound (5) for LSER equation were explained by the following Eq. (8) including quadratic and interactive effects of solvent parameters:

$$\begin{aligned}\nu = \nu_0 &+ k_1\pi^* + k_2\delta + k_3\alpha + k_4\beta + k_{11}\pi^{*^2} + k_{22}\delta^2 + k_{33}\alpha^2 \\ &+ k_{44}\beta^2 + k_{12}\pi^*\delta + k_{13}\pi^*\alpha + k_{14}\pi^*\beta + k_{23}\delta\alpha + k_{24}\delta\beta \\ &+ k_{34}\alpha\beta\end{aligned} \tag{8}$$

where the predicted frequency (ν) was correlated to the intercept (ν_0), linear (k_1, k_2, k_3, k_4), quadratic (k_{11}, k_{22}, k_{33},k_{44}) and interaction (k_{12}, k_{13}, k_{14}, k_{23}, k_{24}, k_{34}) coefficients. The linear, quadratic and interaction coefficients of the respective effects were represented by k and were determined by applying a Student's *t*-test. The Minitab 19 was used for graphical analysis and multi-linear regression of the stretching vibrational frequencies. The regression coefficients, standard deviations of each coefficient, P values and t values for all the linear, interaction and quadratic effects of the parameter determined from analysis of the data was displayed in Table 5 for LSER equation.

As can be seen from Table 5, the ν(C=N)$_2$ of compound (4) and the ν(C=S)$_1$, ν(C=S)$_2$ and ν(C=N)$_1$ of compound (5) respond to the quadratic and interaction effects of solvent parameter. The coefficients of determination (0.9605 for ν(C=N)$_2$ of compound (4) and 0.9501 for (C=S)$_1$, 0.9548 for (C=S)$_2$ and 0.9692 for ν(C=N)$_1$ of compound (5)) obtained from the model containing the linear, interaction and quadratic effects are bigger than that of the linear model (0.9247 for ν(C=N)$_2$ of compound (4) and 0.8660 for (C=S)$_1$, 0.9142 for (C=S)$_2$ and 0.8965 for ν(C=N)$_1$ of compound (5)) given in Table 2 and Table 3. Therefore, it was found that the model including the linear, quadratic and interaction effects for LSER is the most appropriate model for the ν(C=N)$_2$ of compound (4) and the ν(C=S)$_1$, ν(C=S)$_2$ and ν(C=N)$_1$ of compound (5) and shows a better correlation compared to the linear model for LSER.

According to the multi-linear regression analysis, reduced regression equations for the ν(C=N)$_2$ of compound (4) in Eq. (9) and the ν(C=S)$_1$, ν(C=S)$_2$ and ν(C=N)$_1$ of compound (5) is given in Eqs. (10)–(12):

$$\nu_{(C=N)_2} = 1599.68 - 7.08\pi^* + 17.20\alpha - 5.36\beta - 42.80\alpha\pi^* \tag{9}$$

Table 5
Regression model results for LSER equation.

Term	Coefficient	Standard Error	t	F	P	R^2
Compound (4)						
$\nu(C{=}N)_2$						0.9605
Constant	1599.68	0.89	1790.07	48.65	0.000	
π^*	−7.08	1.50	−4.71	22.2	0.002	
α	17.20	8.44	2.04	4.16	0.076	
β	−5.36	1.52	−3.53	12.44	0.008	
$\alpha\pi^*$	−42.80	15.90	−2.07	7.27	0.027	
Compound (5)						
$\nu(C{=}S)_1$						0.9504
Constant	1349.05	1.35	997.9	38.31	0.000	
π^*	−10.77	2.21	−4.87	23.73	0.001	
α	−26.6	6.53	−4.08	16.61	0.004	
β	−13.09	2.59	−5.36	28.75	0.001	
$\alpha\beta$	31.48	8.53	3.69	13.61	0.006	
$\nu(C{=}S)_2$						0.9548
Constant	1317.40	0.95	1391.5	42.27	0.000	
π^*	−5.02	1.59	−3.15	9.95	0.013	
α	18.06	8.94	2.02	4.08	0.078	
β	−5.34	1.61	−3.31	10.97	0.011	
$\alpha\pi^*$	−45.20	16.80	−2.68	7.19	0.028	
$\nu(C{=}N)_1$						0.9692
Constant	1619.08	0.66	2449.1	62.93	0.000	
π^*	−3.87	1.11	−3.48	12.11	0.008	
α	23.59	6.25	3.78	14.26	0.005	
β	−6.58	1.13	−5.84	34.16	0.000	
$\alpha\pi^*$	−51.10	11.80	−4.35	18.89	0.002	

The unit of the stretching vibrational frequency is cm^{-1}.

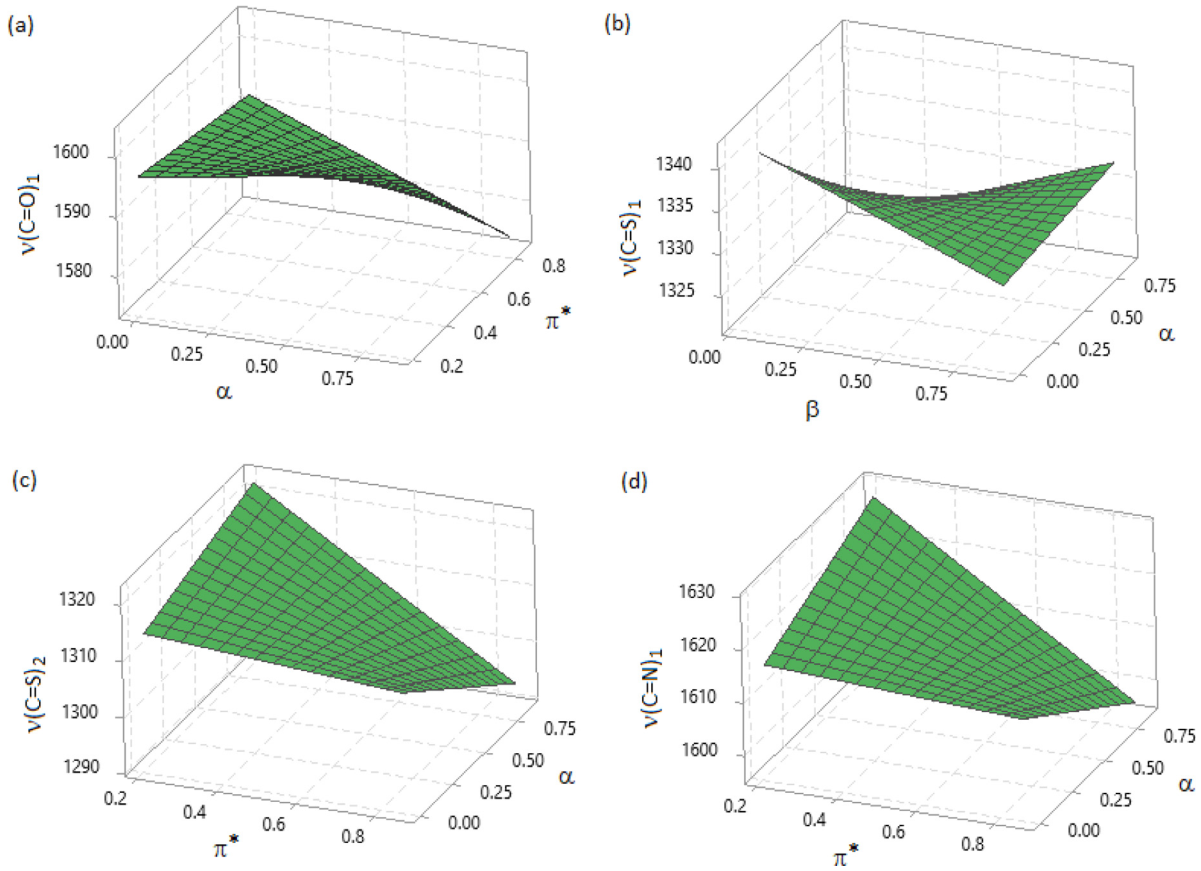

Fig. 8. 3D surface plot for a combined effect of **(a)** α and π^* for the $\nu(C{=}O)_1$ of compound (4) and **(b)** α and β for the $\nu(C{=}S)_1$, **(c)** α and π^* for the $\nu(C{=}O)_2$ and **(d)** α and π^* for the $\nu(C{=}N)_1$ of compound (5).

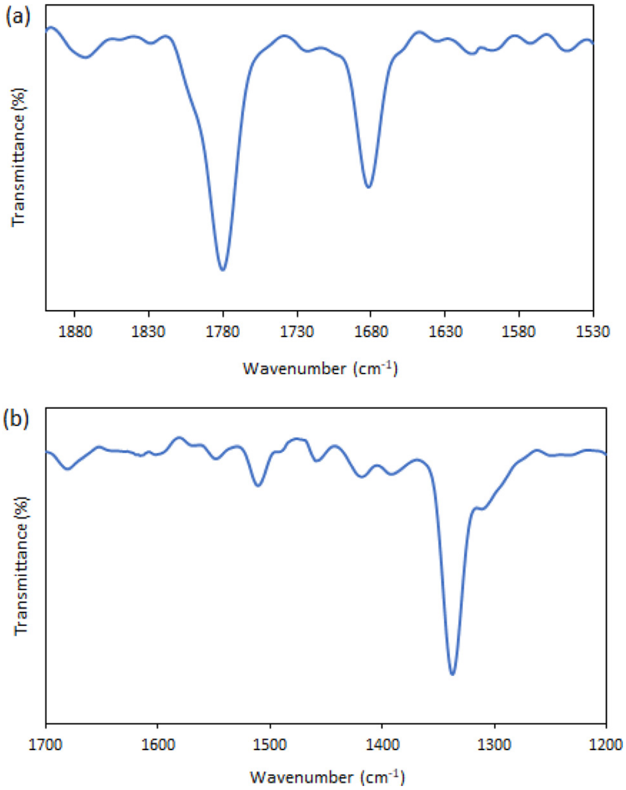

Fig. 9. FT-IR spectra of compound (4) and compound (5) in chlorobenzene.

$$\nu_{(C=S)_1} = 1349.05 - 10.77\pi^* - 26.60\alpha - 13.90\beta + 31.48\alpha\beta \quad (10)$$

$$\nu_{(C=S)_2} = 1317.40 - 5.02\pi^* + 18.06\alpha - 5.34\beta - 45.20\alpha\pi^* \quad (11)$$

$$\nu_{(C=N)_1} = 1619.80 - 3.87\pi^* + 23.59\alpha - 6.58\beta - 51.10\alpha\pi^* \quad (12)$$

It was found that the linear effect of π^* (P = 0.002) and β (P = 0.008) excluding α (P = 0.076), and interaction effect of $\alpha\pi^*$(P = 0.027) on the ν(C═N)$_2$ of compound (4) are highly significant. Additionally, it was determined that linear effect of π^* (P = 0.001 for ν(C═S)$_1$, P = 0.013 for ν(C═S)$_2$ and P = 0.008 for ν(C═N)$_1$), β (P = 0.001 for ν(C═S)$_1$, P = 0.011 for ν(C═S)$_2$ and P = 0.000 for ν(C═N)$_1$) and α (P = 0.004 for ν(C═S)$_1$ and P = 0.005 for ν(C═N)$_1$ excluding ν(C═S)$_2$ with P = 0.078) are highly significant. Interaction effects of $\alpha\beta$ (P = 0.006) on the ν(C═S)$_1$, $\alpha\pi^*$(P = 0.028) on the ν(C═S)$_2$ and $\alpha\pi^*$(P = 0.02) on the ν(C═N)$_1$ of compound (5) are highly significant. The interactive effects of $\alpha\beta$ and $\alpha\pi^*$for LSER equation were represented in form of 3D surface plots in Fig. 8. The interactive effect of $\alpha\beta$ and $\alpha\pi^*$on the ν(C═N)$_2$ of compound (4) and ν(C═S)$_1$, ν(C═S)$_2$ and ν(C═N)$_1$ of compound (5) was the most significant effect and the results are different from that obtained from LSER equation including the linear effects. Therefore, the model containing the linear, interaction and quadratic effects of the parameters could be effectively used to investigate the solvent effects on the ν(C═O)/ν(C═N) of compound (4) and the ν(C═S)/ν(C═N) of compound (5).

4.3. The validation of the model including the linear, quadratic and interaction effects for SE and LSER

The validation of the model including the linear, interaction and quadratic effects for SE and LSER was investigated for the related stretching vibrational frequencies of compound (4) and compound (5) in chlorobenzene. Fig. 9(a) and Fig. 9(b) display the experimental FT-IR spectra of compound (4) and compound (5) in chlorobenzene. Solvent parameters and the experimental/calculated stretching vibrational frequencies of compounds were given in Table 6. It was found that the models including the linear, quadratic and interaction effects for SE and LSER show a better correlation compared to the linear model for SE and LSER.

5. Conclusions

The solvent effects on the ν(C═O)/ν(C═N) of compound (4) and the ν(C═S)/ν(C═N) of compound (5) in 13 different pure solvents are studied by FT-IR experiments and density functional theory calculations using the potential energy distribution (PED) contributions. The results of this study are;

i. Two novel 1,2,4-oxadiazole derivative compounds were synthesized and characterized by IR, ^{1}H NMR, ^{13}C NMR and HRMS analyses.
ii. The observed FT-IR spectra of compound (4) and compound (5) are compared with their theoretical wavenumbers (scaled).
iii. The ν(C═O)/ν(C═N) of compound (4) and the ν(C═S)/ν(C═N) of compound (5) were correlated with the Swain, AN, KBM, and LSER solvent scales.
iv. It was found that the KBM and the solvent ANs of the solvents with the stretching vibrational frequencies compound (4) and compound (5) have poor correlations.
v. The ν(C═O)/ν(C═N) of compound (4) and the ν(C═S)/ν(C═N) of compound (5) achieve good linear correlation with the SE while the LSER equation shows excellent correlation analysis results for the ν(C═O)/ν(C═N) of compound (4) and the ν(C═S)/ν(C═N) of compound (5) in all solvents.

Table 6
The experimental and the calculated stretching vibrational frequencies of compound (4) and compound (5) in chlorobenzene.

Compound and functional group	The stretching vibrational frequencies of compound (4) and compound (5)					β	α	π^*	A_j	B_j
	Experimental	SE (linear effect)	LSER (linear effect)	SE (linear, quadratic and interaction effects)	LSER (linear, quadratic and interaction effects)					
Chlorobenzene						0.07	0.00	0.68	0.20	0.65
Compound (4)										
ν(C═O)$_1$	1780.94	1782.37	1780.78	1780.93						
ν(C═N)$_1$	1612.14	1614.84	1614.69							
ν(C═N)$_2$	1594.49	1594.05	1593.78		1594.49					
Compound (5)										
ν(C═S)$_1$	1341.05	1338.91	1339.17		1340.75					
ν(C═S)$_2$	1313.94	1312.87	1312.86		1313.61					
ν(C═N)$_1$	1616.11	1615.67	1615.87		1616.71					
ν(C═N)$_2$	1602.79	1603.79	1603.79	1602.45						

The unit of the stretching vibrational frequency is cm^{-1}.

vi. The LSER equation allows the prediction of the $\nu(\mathrm{C{=}O})/\nu(\mathrm{C{=}N})$ of compound (4) and the $\nu(\mathrm{C{=}S})/\nu(\mathrm{C{=}N})$ of compound (5) in other solvents if the LSER parameters of these solvents are known.
vii. The solvent effects on the $\nu(\mathrm{C{=}O})/\nu(\mathrm{C{=}N})$ of compound (4) and the $\nu(\mathrm{C{=}S})/\nu(\mathrm{C{=}N})$ of compound (5) for SE and LSER were investigated by QE including quadratic and interactive effects of solvent parameters:
viii. In order to predict the $\nu(\mathrm{C{=}O})/\nu(\mathrm{C{=}N})$ of compound (4) and the $\nu(\mathrm{C{=}S})/\nu(\mathrm{C{=}N})$ of compound (5) in chlorobenzene, QE were applied for SE and LSER equation. The model including the linear, quadratic and interaction effects provided more accurate predictions than SE and LSER equations including linear effects.

CRediT authorship contribution statement

Yesim S. Kara: Investigation, Writing - original draft, Writing - review & editing. **Mustafa Ünsal:** Investigation. **Nalan Tekin:** Data curation, Methodology, Writing - review & editing. **Aslı Eşme:** Data curation, Methodology, Writing - review & editing.

Declaration of Competing Interest

The authors declare that they have no known competing financial interests or personal relationships that could have appeared to influence the work reported in this paper.

Acknowledgement

This work was supported by Kocaeli University Scientific Research Projects Coordination Unit. under Project Number 2255.

Appendix A. Supplementary material

Supplementary data to this article can be found online at https://doi.org/10.1016/j.saa.2020.119424.

References

[1] P. Pitasse-Santos, V. Sueth-Santiago, M.E.F. Lima, 1,2,4- and 1,3,4-oxadiazoles as scaffolds in the development of antiparasitic agents, J. Braz. Chem. Soc. 29 (3) (2018) 435–456.
[2] D.C. Pevear, T.M. Tull, M.E. Seipel, J.M. Groarke, Activity of pleconaril against enteroviruses, Antimicrob. Agents Chemother. 43 (9) (1999) 2109–2115.
[3] K. Axel, E. Jürgen, Pharmaceutical Substances: Syntheses, Patents, Applications. Thieme Chemistry, Stuttgart, Germany, 2001.
[4] D. Kumar, G. Patel, A.K. Chavers, K.-H. Chang, K. Shah, Synthesis of novel 1,2,4-oxadiazoles and analogues as potential anticancer agents, Eur. J. Med. Chem. 46 (7) (2011) 3085–3092.
[5] J.W.H. Watthey, M. Desai, R. Rutledge, R. Dotson, Synthesis and diuretic profile of 3-(3-amino-1,2,4-oxadiazol-5-yl)-5-chloro2,6-pyrazinediamine, an amiloride-type diuretic, J. Med. Chem. 23 (1980) 690–699.
[6] F.J. Swinbourne, J.H. Hunt, G. Klinkert, Advances in indolizine *chemistry*, Adv. Heter. Chem. 23 (1979) 103–170.
[7] C.V. Maftei, E. Fodor, P.G. Jones, C.G. Daniliuc, M.H. Franz, G. Kelter, H.H. Fiebig, M. Tamm, I. Neda, Novel bioactive 1,2,4-oxadiazole natural product analogs. synthesis, structural analysis and potential antitumor activity, Rev. Roum. Chim. 60 (1) (2015) 75–83.
[8] E. Rajanarendar, S. Raju, M.N. Reddy, K.R. Murthy, An elegant one-pot synthesis of isoxazolo[2,3-a]pyrimidines, Indian J. Chem. 49B (2010) 1422–1427.
[9] Ş. Yurdakul, S. Tanrıbuyurdu, Theoretical and experimental study of solvent effects on the structure, vibrational spectra, and tautomerism of 3-amino-1,2,4-triazine, J. Mol. Struct. 1052 (2013) 57–66.
[10] N. Tekin, H. Namlı, O. Turhan, Solvents effect on infrared spectra of 1,3-indanedione in organic solvents, Vib. Spectrosc. 39 (2005) 214–219.
[11] H.R. Kricheldorf, ^{15}N NMR spectroscopy acids: 7†—solvent effects on α-and ω-amino, Org. Magn. Resonance 12 (7) (1979) 414–417.
[12] M.C. Almandoz, M.I. Sancho, P.R. Duchowicz, S.E. Blanco, UV-Vis spectroscopic study and DFT calculation on the solvent effect of trimethoprim in neat solvents and aqueous mixtures, Spectrochim. Acta A-M. 129 (2014) 52–60.
[13] L. Beyere, S. Yarasi, G.R. Loppnow, Solvent effects on sunscreen active ingredients using Raman spectroscopy, J. Raman Spectrosc. 34 (2003) 743–750.
[14] S.M. Khopde, K.I. Priyadarsini, D.K. Palit, T. Mukherjee, Effect of solvent on the excited-state photophysical properties of curcumin, Photochem. Photobiol. 72 (5) (2000) 625–631.
[15] Y. Li, H. Zhang, Q. Liu, FT-IR spectroscopy and DFT calculation study on the solvent effects of benzaldehyde in organic solvents, Spectrochim. Acta A-M. 86 (2012) 51–55.
[16] Q. Liu, C. Cong, H. Zhang, Investigation on infrared spectra of androsterone in single solvents, Spectrochim. Acta A-M. 68 (2007) 1269–1273.
[17] X. Ji, Y. Li, J. Zheng, Q. Liu, Solvent effects of ethyl methacrylate characterized by FTIR, Mater. Chem. Phys. 130 (2011) 1151–1155.
[18] H. Song, H. Zhang, H. Yang, Q. Liu, FTIR spectral studies of methyltestorone in single and binary solvent systems, Spectrochim. Acta A. 72 (2009) 709–714.
[19] Y. Chen, H. Zhang, W. Zhou, C. Deng, J. Liao, The solvent effects on dimethyl phthalate investigated by FTIR characterization, solvent parameter correlation and DFT computation, Spectrochim. Acta A-M. 199 (2018) 412–420.
[20] V. Gutmann, G. Resch, The Donor-Acceptor Interactions, Plenum Press, New York, 1978, p. 29.
[21] J.G. Kirkwood, Theory of solutions of molecules containing widely separated charges with special application to zwitterions, J. Chem. Phys. 2 (1934) 351–361.
[22] E. Bauer, M. Magat, Deformation of molecules in condensed phases and the hydrogen bond, J. Physique Radium 9 (1938) 319–330.
[23] C.G. Swain, M.S. Swain, A.L. Powell, S. Alunni, Solvent effects on chemical reactivity, evaluation of anion and cation solvation components, J. Am. Chem. Soc. 105 (1983) 502–513.
[24] M.J. Kamlet, J.-L.-M. Abboud, M.H. Abraham, R.W. Taft, Linear solvation energy relationships. 23. A comprehensive collection of solvatochromic parameters π^*, α, and β, and some methods for simplifying the generalized solvatochromic equation, J. Org. Chem. 48 (1983) 2877–2887.
[25] Y. Chen, H. Zhang, Q. Liu, FT-IR spectroscopy combined with DFT calculation to explore solvent effects of vinyl acetate, Spectrochim. Acta A-M. 126 (2014) 122–128.
[26] I. Ajaj, J. Markovski, M. Rančić, D. Mijin, M. Milčić, M. Jovanović, A. Marinković, Solvent and structural effects in tautomeric 2(6)-hydroxy-4-methyl-6(2)-oxo-1-(substituted phenyl)-1,2(1,6)-dihydropyridine-3-carbonitriles: UV, NMR and quantum chemical study, Spectrochim. Acta A. 150 (2015) 575–585.
[27] R.A. Nyquist, H.A. Fouchea, G.A. Hoffman, D.L. Hasha, Infrared study of β-propiolactone in various solvent systems and other lactones, Appl. Spectrosc. 45 (1991) 860–867.
[28] Q. Liu, W. Sang, X. Xu, Solvent effects on infrared spectra of 5-methyl-7-methoxy-iso-flavone in single solvent systems, J. Mol. Struct. 608 (2002) 253–257.
[29] Y. Dürüst, C. Altuğ, F. Kılıç, Thiophene-substituted 1, 2, 4-oxadiazoles and oxadiazines, Phosphorus, Sulfur Relat. Elem. 182 (2007) 299–313.
[30] M.J. Frisch, G.W. Trucks, H.B. Schlegal, G.E. Scuseria, M.A. Robb, J.R. Cheesman, V. G.; Zakrzewski, J.A. Jr.Mortgomerg, R.E. Stratmann, J.C. Burant, et al. Gaussian 09, Revision A.1; Gaussian Inc.: Wallingford CT, 2009.
[31] A.D. Becke, Density-functional thermochemistry. III. The role of exact exchange, J. Chem. Phys. 98 (1993) 5648–5652.
[32] C. Lee, W. Yang, R.G. Parr, Development of the Colle-Salvetti correlation-energy formula into a functional of the electron density, Phys. Rev. B: Condens. Matter 37 (1988) 785–789.
[33] T. Keith, J. Millam, GaussView, Version 5.0.9; Semichem. Inc.: Shawnee Mission KS, 2009.
[34] M.H. Jamroz, Vibrational Energy Distribution Analysis VEDA 4, Warsaw, 2004.
[35] J.A. Pople, H.B. Schlegel, R. Krishnan, D.J. Defrees, J.S. Binkley, M.J. Frisch, R.A. Whiteside, R.F. Hout, W.J. Hehre, Molecular orbital studies of vibrational frequencies, Int. J. Quantum Chem. 15 (1981) 269–278.
[36] G. Varsányi, Vibrational Spectra of Benzene Derivatives, first ed., Elsevier Science, Burlington, NJ, USA, 2012.
[37] G. Varsányi, L. Láng, Assignments for vibrational spectra of seven hundred benzene derivatives, Wiley:, New York, NY, USA, 1974.
[38] S. Bee, P. Agarwal, A. Gupta, P. Tandon, Use of vibrational spectroscopy to study 2-[4-(N-dodecanoylamino)phenyl]-5-(4-nitrophenyl)-1,3,4-oxadiazole: a combined theoretical and experimental approach, Spectrochim. Acta A 114 (2013) 236.
[39] R.M. Silverstein, F.X. Webstor, Spectrometric Identification of Organic Compounds, sixth ed., John Wiley & Sons, New York, 1998.
[40] B. Jović, A. Nikolić, S. Petrović, B. Kordić, T. Đaković-Sekulić, N. Stojanović, FTIR investigation of solvent effects of N-methyl and N-tert-butyl benzamide, J. Struct. Chem. 55 (8) (2014) 1616–1622.
[41] C. Parlak, M. Tursun, C.S.C. Kumar, D. Bilge, N. Kazanci, L. Rhyman, P. Ramasami, Halogen and solvent effects on the conformational, vibrational and electronic properties of 1,4-diformylpiperazine: a combined experimental and DFT study, J. Theor. Comput. Chem. 14 (7) (2015) 1550050.
[42] M. Tursun, C. Parlak, Conformation stability, halogen and solvent effects on C=O stretching of 4-chloro-3-halogenobenzaldehydes, Spectrochim. Acta A-M. 141 (2015) 58–63.
[43] S.M. Rafigha, A.V. Yazdia, M. Vossoughib, A.A. Safekordia, M. Ardjmand, Optimization of culture medium and modeling of curdlan production from Paenibacillus polymyxa by RSM and ANN, Int. J. Biol. Macromol. 70 (2014) 463–473.